Abrupt onset of the capillary-wave spectrum at wall-fluid interfaces

A.O. Parry[1] and C. Rascón[2]

[1] *Department of Mathematics, Imperial College London, London SW7 2BZ, UK*

[2] *GISC, Departamento de Matemáticas, Universidad Carlos III de Madrid, 28911 Leganés, Madrid, Spain*

Surfaces between 3D solids and fluids exhibit a wide variety of phenomena both at equilibrium, such as roughening transitions, interfacial fluctuations and wetting, and also out-of-equilibrium, such as the surface growth of driven interfaces. These phenomena are described very successfully using lower dimensional (2D) effective models which focus on the physics associated with emergent mesoscopic lengths scales, parallel to the interface, where the 2D-like behaviour is physically transparent. However, the precise conditions under which this dimensional reduction is justifiable have remained unclear. Here we show that, for a wall-fluid interface, a dimensional reduction from 3D-like to 2D-like behaviour – identified via the decay of density correlations – occurs abruptly at a specific value of the contact angle, and indicates the beginning of interfacial-like 2D behaviour and the spontaneous onset of the capillary-wave spectrum. The reduction from 3D to 2D is characterised by the divergence of a correlation length perpendicular to the interface revealing a morphological change in the nature of density correlations. Counter-intuitive effects occur, including that 3D behaviour can persist up to the wetting temperature and also that 2D behaviour can begin when no wetting layer is present and the adsorption is negative.

Many 3D systems exhibit behaviour that can be described very successfully by lower dimensional (2D) effective models. Celebrated examples of these include studies of the Capillary Wave model of thermally induced fluctuations in the interfacial region separating coexisting liquid and gas phases [1, 2], and also roughening [3] and wetting transitions [4, 5]. Understanding the emergence of such 2D-like behaviour poses some of the most challenging problems in the statistical mechanical theory of interfaces. Indeed, although such crossover from 3D to 2D is ubiquitous for structural properties and also in determining the location of phase boundaries, often only scaling or phenomenological criteria are available. For example, the use of the Capillary Wave model in the description of both the interfacial region and wetting transitions is usually justified when the emergent parallel correlation length is "*much larger*" than an underlying microscopic length scale, typically the bulk correlation length. Attempts to understand this crossover and the emergence of interfacial behaviour are the subject of much current research and have been controversial for decades [6–9].

Here we show that the nature of the 3D/2D crossover and the mechanism for the onset of interfacial behaviour can be understood in detail for wall-fluid interfaces through *abrupt* structural changes in the decay of density correlations. We build on the pioneering microscopic treatments of wetting due to Cahn [10], and Nakanishi and Fisher [11], but focus attention on the correlation function structure over the whole range of wetting layer thicknesses. Following these authors, our study is based on a simple square-gradient density functional model of fluid adsorption in systems with short-ranged forces near a wall situated in the $z = 0$ plane. Adopting a magnetic notation, with local order-parameter $m(\mathbf{r})$, the free-energy functional is written

$$F[m] = \int d\mathbf{r} \ \left\{ \frac{1}{2}(\nabla m)^2 + \phi(m) \right\} + \int d\mathbf{x} \ \phi_1(m_1) \tag{1}$$

where $\phi(m)$ is a double-well bulk potential and $\phi_1(m) = c\,m^2/2 - h_1 m$ is the surface interaction, which couples to the magnetisation at the wall m_1, via a surface enhancement c and surface field h_1. We restrict attention to sub-critical temperatures $T < T_c$ and, for simplicity, assume an Ising symmetry denoting the bulk spontaneous magnetization m_0 and $\kappa = 1/\xi_b$ the inverse of the bulk correlation length. We begin by supposing that the bulk magnetic field is $h = 0^-$ so that the bulk magnetization takes the value $-m_0$. Minimizing $F[m]$ yields the Euler-Lagrange equation for the equilibrium magnetization profile $m(z)$. An elegant graphical solution (or Cahn construction [10]), based on the well-known analogy with the mechanical conservation of energy [12], determines both $m(z)$ and the Nakanishi-Fisher global surface phase diagrams [11]. These show lines of critical wetting transitions for $c > \kappa$, for which the adsorption, $\Gamma = \int_0^\infty dz \ (m(z) + m_0)$, diverges continuously, and lines of first-order wetting transitions for which the adsorption jumps from a microscopic to a macroscopic value on approaching the wetting temperature T_w (See Fig 1). Here, we focus on the properties of the correlation function $G(\mathbf{r}, \mathbf{r}') = \langle m(\mathbf{r})m(\mathbf{r}')\rangle - m(z)m(z')$ which is best studied via its transverse Fourier transform $G(z, z'; q)$, where $\mathbf{q}$ is a 2D wavevector parallel to the wall with modulus q. This

correlation function satisfies the inhomogeneous Ornstein-Zernike equation [12, 13] and has a spectral expansion

$$G(z,z';q) \;=\; k_BT \,\sum_n \,\frac{\psi_n^*(z)\,\psi_n(z')}{E_n+q^2} \tag{2}$$

with wavefunctions ψ_n and eigenvalues E_n satisfying a Shrödinger-like equation. In general, the spectral sum contains both bound states, for which $E_n < \kappa^2$, and a continuum of scattering states with higher energies. The ground-state is of particular importance since it identifies the true correlation length, determining the asymptotic exponential decay of correlations. If the ground-state is bound ($E_0 < \kappa^2$), the correlation function decays asymptotically as $G(\mathbf{r},\mathbf{r}') \propto e^{-x/\xi_\parallel}/x^{1/2}$ with a parallel correlation length $\xi_\parallel = 1/\sqrt{E_0}$, which is greater than ξ_b. Here, x is the distance parallel to the wall between the points $\mathbf{r}$ and $\mathbf{r}'$. This classic Ornstein-Zernike decay is indicative of 2D-like behaviour arising from interfacial fluctuations. However, if only scattering states exist, such that $E_0 = \kappa^2$, the correlation function, while still inhomogeneous, decays with the bulk 3D correlation length ξ_b in all available directions. We refer to these scenarios as the 2D-like and 3D-like regimes, respectively.

Here, we point out that the correlation function changes abruptly from a 3D-like to a 2D-like regime, corresponding to the spontaneous onset of interfacial-like properties and the capillary wave spectrum, as the adsorption increases, leading to a number of counter-intuitive effects. To see this, we recall that recent studies of free interfaces have revealed that both the correlation function and its integral (the structure factor) display a hierarchy of resonances which constrain greatly their structure [14]. These resonances point to a class of potentials $\phi(m)$ for which the correlation function $G(z,z';q)$ can be determined analytically within square gradient theory, which we extend here to the wall-fluid interface. We illustrate this for the most important case of the standard "m^4" potential $\phi(m) = -\frac{t}{2}m^2 + \frac{u}{4}m^4$, with $t = T_c - T$, for which $m_0 = \sqrt{t/u}$ and $\kappa = \sqrt{2t}$. The eigenvalues E_n are conveniently expressed in terms of the parameter $\tau = m_1/m_0$, which simple measures the surface magnetization, and which is related to c and h_1 via the quadratic relation $\tau^2 - 2\tau\, c/\kappa + 2\, h_1/m_0\,\kappa - 1 = 0$, and satisfy

$$\frac{\sqrt{k^2-E_n}-\kappa\,\tau}{\sqrt{k^2-E_n}+c} = \frac{f(\tau)}{1-\tau^2} \tag{3}$$

where $f(x) = x^2 - 2\sqrt{1-E_n\,\xi_b^2}\;\; x + 1 - \frac{4}{3}E_n\,\xi_b^2$. The spectra of bound states for different values of the surface enhancement c are shown in Fig. 2. A central result of our paper is that bound states (i.e. 2D-like interfacial behaviour) only exist for sufficiently large surface magnetisations $\tau > \tau_*$, where τ_* is determined by $\kappa\,\tau_*(\tau_*^2-1) = c\,(\tau_*^2 - 1/3)$ as follows from (3). This point marks the crossover between the 3D-like and the 2D-like regimes, and the abrupt onset of the capillary-wave spectrum.

As expected, the eigenvalue spectrum has different features for systems showing critical wetting ($c > \kappa$) and first-order wetting (See Fig. 2). The spectrum is simplest for critical wetting: The ground-state energy E_0 is always positive and decreases monotonically from the value $E_0 = \kappa^2$ at $\tau = \tau_*$ to $E_0 = 0$ as τ increases towards unity, corresponding to the critical wetting temperature [15]. We note that the value of τ_* is largest when $c = \infty$ for which $\tau_* = -1/\sqrt{3}$, and decreases to $\tau_* \approx -0.7925$ at $c = \kappa$. For sufficiently thick films, a second bound state E_1 also exists, but this does not affect the asymptotic decay of the correlation function. For $c < \kappa$, however, pertinent to first-order wetting transitions, the spectrum is more involved. In this case, the ground-state E_0 decreases from the value $E_0 = \kappa^2$ at $\tau = \tau_*$ and vanishes at $\tau = \tau_s < 1$, corresponding to a spinodal. For $\tau_s < \tau < 1$, the ground-state E_0 is negative, implying that the thin-film phase is unstable. Prior to the spinodal, a first-order wetting transition occurs at $\tau_w < \tau_s$, determined by the equal areas condition in the Cahn construction. The range $\tau < \tau_w$ corresponds to partial wetting profiles, while these are metastable for $\tau_w < \tau < \tau_s$, in which case the wall is completely wet. However, for first-order wetting, we must distinguish between two different scenarios. For $c > c_\dagger \approx -0.3375\kappa$, the 3D/2D crossover precedes the wetting transition, so that the correlations in the thin film display a 2D-like interfacial character at the wetting transition. For $c < c_\dagger$, on the other hand, the wetting transition *precedes* the crossover (i.e. $\tau_w < \tau_*$) so that, remarkably, the decay of correlations within the thin wetting layer have a 3D character, set by the bulk correlation length ξ_b, all the way up to the wetting temperature.

The loci of the 3D/2D crossover appear as green lines in the Nakanishi-Fisher global surface phase diagrams, separating regions where the decay of the correlations is 2D or 3D-like (see Fig. 1). For $c > 0$, the crossover always occurs for $h_1 < 0$, on the opposite side of the lines of wetting transitions (shown in red and blue), while for $c = 0$ the crossover occurs exactly at $h_1 = 0$, corresponding to a neutral wall. However, for $c < 0$, the lines of crossover and first-order wetting intersect at a point, corresponding to the condition $\tau_* = \tau_w$. Each point on the lines of crossover corresponds to a specific value of the contact angle θ_* determined only by the dimensionless ratio c/κ (See Fig. 3). Provided c is positive, the value of θ_* is large, with a maximum value of $\cos^{-1}\left(-4\sqrt{3}/9\right) \approx 140.3^\circ$ for $c = \infty$,

while, for $c = 0$, as mentioned above, $\theta_* = 90^\circ$ (a neutral wall). However, on making the surface enhancement negative, the value of θ_* rapidly decreases and vanishes at $c = c_\dagger$ according to $\theta_* \propto (c - c_\dagger)^{\frac{1}{2}}$ and remains zero for all $c < c_\dagger$.

The dimensional reduction occurring for surface enhancement $c < 0$ reveals a number of counter-intuitive effects. The first of these, as mentioned above, is that 3D-like behaviour can persist all the way to the wetting temperature. More striking still is that the point of intersection of the lines of first-order wetting and dimensional reduction correspond to the surface magnetization parameter $\tau \approx -1.1327$, implying the the adsorption Γ is still *negative*, i.e. the 3D/2D crossover occurs when there is no discernible wetting layer at T_w. Consequently (see Fig. 4), the line of first-order wetting transitions in the surface phase diagram for $c < 0$ divides into three sections depending on the value of the wetting temperature T_w: i) For $T_c > T_w > T_{\rm DR}$, the adsorption at the phase boundary is negative and correlations are 3D-like, ii) For $T_{\rm DR} > T_w > T_{\Gamma=0}$, the adsorption is negative and correlations are 2D-like, with $\xi_\parallel > \xi_b$, iii) For $T_{\Gamma=0} > T_w$, the adsorption is positive and correlations are 2D-like, with $\xi_\parallel > \xi_b$. The dimensional reduction occurring at $T_{\rm DR}$ happens when $c \approx -0.3375\,\kappa$ (at which $\xi_\perp^{\rm MF} = \infty$ and $\xi_\parallel = \xi_b$), while the adsorption changes sign at $T_{\Gamma=0}$, when $c = (1 - 2^{1/3})\,\kappa$ (at which $\xi_\perp^{\rm MF} \approx 3.85\,\xi_b$ and $\xi_\parallel \approx 1.04\,\xi_b$), indicating that fluctuations, while 2D-like, have a prominent tubular character. Since, at mean-field level, we may assume that $\kappa \propto (T_c - T_w)^{1/2}$, it follows that the temperatures $T_{\rm DR}$ and $T_{\Gamma=0}$ satisfy

$$\frac{T_c - T_{\rm DR}}{T_c - T_{\Gamma=0}} \;\approx\; 0.5931 \tag{4}$$

which does not depend on any parameters. Such counter-intuitive effects do not occur for $c \geq 0$, as pertinent to wetting in simple fluids, for which the adsorption is always positive and the correlations are always 2D-like at the wetting transition. The case of negative surface enhancement may be realizable for wetting in complex fluids or, equivalently, for surface-induced disorder phenomena in magnets. Regardless of the sign of c, far from T_c, the line of first-order wetting transitions occurs along $h_1 \approx 0.3406\,\kappa\, m_0$ at which the microscopic adsorption if positive and the correlation function 2D-like with anisotropic correlation lengths with universal $\kappa\,\xi_\perp^{\rm MF} \approx 1.544$ and $\kappa\,\xi_\parallel \approx 1.3121$.

As the free-energy remains analytic, the abrupt 3D/2D crossover occuring at τ_* corresponds to a non-thermodynamic singularity. Nevertheless, it is characterised by critical singularities and diverging length scales which, surprisingly, are identical to those occurring at a wetting transition in a lower dimension. To see this, we note that the mechanism for the vanishing of the bound state $\psi_0(z)$ as τ approaches τ_* is precisely the same as that for the ground-state wavefunction in the continuum transfer matrix treatment of 2D short-ranged wetting [16]. This implies that the eigenvalue E_0 approaches the band of scattering states as $\kappa^2 - E_0 \propto (\tau - \tau_*)^2$, displaying the same singularity as the excess free-energy at 2D wetting transitions, with $\tau - \tau_*$ replacing $T_w^{\rm 2D} - T$. Even more surprising, the bound-state wave-function $\psi_0(z)$ becomes diffuse as $\tau \to \tau_*$ and, for distances $z \gg \xi_b$, decays as $\psi_0(z) \approx e^{-z/\xi_\perp^{\rm MF}}$ containing a large perpendicular correlation length which, *even at mean-field level*, diverges as $\xi_\perp^{\rm MF} \approx (\tau - \tau_*)^{-1}$. This divergence displays the exact same critical behaviour as that of the adsorption and roughness for 2D short-ranged critical wetting [17]. We stress, however, that the interpretation of the divergence of $\xi_\perp^{\rm MF}$ for the 2D/3D crossover is very different from the interfacial wandering occurring at 2D wetting transitions. For $\tau > \tau_*$, the asymptotic real space decay of the correlation function for large transverse separations $x \gg \xi_\parallel$, takes the form

$$G(\mathbf{r}, \mathbf{r}') \propto \frac{1}{\left(\xi_\perp^{\rm MF}\right)^2}\; e^{-(z+z')/\xi_\perp^{\rm MF}}\;\; \frac{e^{-x/\xi_\parallel}}{x^{1/2}} \tag{5}$$

where the mean-field perpendicular and parallel correlation lengths are related *exactly* by

$$\left(\frac{1}{\xi_\perp^{\rm MF}}\right)^2 + \left(\frac{1}{\xi_\parallel}\right)^2 = \left(\frac{1}{\xi_b}\right)^2 \tag{6}$$

This expression makes clear that the divergence of $\xi_\perp^{\rm MF}$ is not related to interfacial fluctuations, and must not be confused with a capillary-wave induced interfacial roughness $\xi_\perp \propto \sqrt{\ln \xi_\parallel}$, which is absent in our mean-field model. On approaching τ_*, the perpendicular correlation length $\xi_\perp^{\rm MF}$ diverges, while the parallel correlation length $\xi_\parallel \to \xi_b$, implying that the dimensional crossover is associated with the growth of pseudo one-dimensional tubes or spikes which tunnel away from the wall and penetrate progressively further into the bulk. The divergence of $\xi_\perp^{\rm MF}$ provides the mechanism by which the isotropy of the asymptotic exponential decay of the correlation function is recovered in the 3D regime. We note, however, that the singular contribution (5) to the correlation function arising from these pseudo one-dimensional fluctuations *vanishes* at the 2D/3D crossover, where they are consumed within the scattering states. Such tube-like fluctuations have been long speculated to be the origin of the Ornstein-Zernike decay of the

correlation function in 3D [18], and provide the mechanism by which separate interfaces communicate in systems with short-ranged forces [19].

We believe that the above predictions remain valid beyond mean-field, although there may be an additional signature of the dimensional crossover in the decay of the magnetization profile $m(z)$. We anticipate that this is weak in 3D, where only the amplitude of the exponential decay $m(z) + m_0 \propto e^{-\kappa z}$ is altered due to the onset of interfacial fluctuations for $\tau > \tau_*$, but is much stronger in lower dimensions. Support for this comes from studies of the 2D Ising model, for which exact results are available. Abraham and Huse studied the asymptotic decay of the magnetization profile in a semi-infinite Ising model with a surface field h_1 (and surface enhancement $c = 0$, since the bond strength is not altered at the surface) [20]. For this model, the above mean-field theory predicts that a dimensional crossover associated with a qualitative change in the nature of fluctuations due to the onset of the capillary wave spectrum occurs at $h_1 = 0$ (corresponding to $\theta_* = 90^\circ$). Abraham and Huse show that, for $T < T_c$ and bulk field $h = 0^-$, the profile indeed exhibits different asymptotic decays, depending on the sign of h_1. For all $h_1 < 0$, the profile decays as $m(z) + m_0 \approx e^{-z/\xi_b}/z^{\frac{3}{2}}$, where $\xi_b/k_BT = (2\gamma)^{-1}$ is the bulk correlation length and γ is the surface tension. However, for all $h_1 > 0$, the profile decays as $m(z) + m_0 \approx e^{-z/\xi_\perp}$, involving a larger perpendicular correlation length arising from interfacial fluctuations. Moreover, Abraham and Huse show that this crossover is associated with a morphological change in the dominant droplet contributions to the partition function which are tubular-like for $h_1 < 0$, but triangular for $h_1 > 0$, where they meet the wall at the equilibrium contact angle, identifying that $\xi_\perp = \xi_b/\sin\theta$ (provided $\theta < 90^\circ$). The location of this crossover is therefore unchanged from the mean-field prediction.

Our predictions for the dimensional crossover can be tested in a number of ways. Although the direct measurement of the correlation function is possible in principle, it may be easier to study the magnetization profile in geometries which break the translational invariance along the wall. This is analogous to the Fisher-Widom non-thermodynamic singularity, where the decay of the bulk correlation function changes from being oscillatory to monotonic [21], which is also observable through the decay of the density profile at a liquid-gas interface [22]. Similarly, for a planar wall with a small protrusion or step (say) near $x = 0$, the magnetization profile $m(x, z)$ will decay towards the planar profile $m(\infty, z) = m(z)$ as the distance x from the step increases. The perturbation from the planar value, $\delta m(x, z) = m(x, z) - m(z)$ has a series expansion solution $\delta m = \sum_n \alpha_n \psi_n(z)\, e^{-\sqrt{E_n}\, x}$, using the same complete set of eigenfunctions appearing in the correlation function (2). It follows that the asymptotic decay is different either side of the 2D/3D crossover, behaving as

$$\delta m(x, z) \;\propto\; \begin{cases} e^{-z/\xi_\perp^{\rm MF}} \cdot e^{-x/\xi_\parallel} & \text{for } \tau > \tau_* \\ z\, e^{-x/\xi_b} & \text{for } \tau < \tau_* \end{cases} \tag{7}$$

which highlights that the perpendicular correlation length $\xi_\perp^{\rm MF}$ is observable in the asymptotic decay, but is not present in the planar profile $m(\infty, z)$. Similar crossover will occur at wedges or chemically patterned walls [23].

The counter-intuitive behaviour highlighted above cannot be (easily) described using 2D interfacial models based on a collective coordinate $\ell(\mathbf{x})$ representing the wetting layer thickness. This is obviously the case in regime i) of Fig. 4, where the correlation function at the wetting transition is 3D-like. However, even in regimes ii) and iii), where correlations and fluctuations are 2D-like, one cannot define consistently an interfacial coordinate $\ell(\mathbf{x})$ since, at $T_{\Gamma=0}$, the profile is completely flat ($m(z) = -m_0$) and fluctuations about it cannot be described by the translations of an intrinsic or constrained profile [24]. The properties of the correlation function for $c < 0$ and the results (4) appear to be beyond the reach of all interfacial models. Finally, we mention that the wall-liquid interface will show additional correlation function structure arising from volume exclusion for more realistic fluid models. For example, within the 3D regime, where the lateral decay of the correlation function is determined by the bulk *liquid* correlation length ξ_l, there may be an additional non-thermodynamic singularity associated with the Fisher-Widom line [21]. Molecular layering and thin-thick transitions, which are present in some models of wall-fluid interfaces, will also enrich the correlation function structure.

Methods

The theoretical methods employed in this paper, including the determination of the spectrum E_n and the eigenfunctions $\psi_n(z)$, can be found in the Supplementary Material. The data for the figures was computed using standard numerical methods.

Acknowledgments

CR acknowledges the support of the grant PID2021-126307NB-C21/AEI/10.13039/501100011033/FEDER,UE.

Author Contributions

A.O.P. conceived problem and subsequent joint theoretical development. C.R. performed joint theoretical development and numerical computations.

Competing Interests statement

None

[1] F. P. Buff, R. A. Lovett, and F. H. Stillinger, Interfacial Density Profile for Fluids in the Critical Region, Phys. Rev. Lett. **15**, 621–623 (1965).
[2] D. G. A. L. Aarts, M. Schmidt, and H. N. W. Lekkerkerker, Direct visual observation of thermal capillary waves, Science **304**, 847 (2004).
[3] S. T. Chui and J. D. Weeks, Dynamics of the Roughening Transition, Phys. Rev. Lett. **40**, 733 (1978).
[4] E. Brézin, B. I. Halperin, and S. Leibler, Critical Wetting in Three Dimensions, Phys. Rev. Lett. **50**, 1387 (1983).
[5] A. Squarcini, J. M. Romero-Enrique, and A. O. Parry, Casimir Contribution to the Interfacial Hamiltonian for 3D Wetting, Phys. Rev. Lett. **128**, 195701 (2022).
[6] C. Fradin, A. Braslau, D. Luzet, D. Smilgies, M. Alba, N. Boudet, K. Mecke, and J. Daillant, Structure and surface energy of liquid interfaces at short length-scales, Nature **403**, 871–874 (2000).
[7] E. Chacón and P. Tarazona, Intrinsic Profiles beyond the Capillary Wave Theory: A Monte Carlo Study, Phys. Rev. Lett. **91**, 166103 (2003).
[8] F. Höfling and S. Dietrich, Enhanced wavelength-dependent surface tension of liquid–vapor interfaces, Europhys. Lett. **109**, 46002 (2015).
[9] A. O. Parry, C. Rascón, and R. Evans, The local structure factor near an interface; beyond extended capillary-wave models , J. Phys.: Condens. Matter **28**, 244013 (2016).
[10] J. W. Cahn, Critical Point Wetting, J. Chem. Phys. **66**, 3667 (1977).
[11] H. Nakanishi and M. E. Fisher, Multicriticality of Wetting, Prewetting, and Surface Transitions, Phys. Rev. Lett. **49**, 1565 (1982).
[12] J. S. Rowlinson and B. Widom, *Molecular Theory of Capillarity* (Clarendon Press, 1982).
[13] R. Evans, The nature of the liquid-vapour interface and other topics in the statistical mechanics of non-uniform, classical fluids, Adv. Phys. **28**, 143 (1979).
[14] A. O. Parry and C. Rascón, The Goldstone mode and resonances in the fluid interfacial region , Nature Physics **15**, 287–292 (2019).
[15] E. Brézin, B. I. Halperin, and S. Leibler, Critical Wetting - The Domain of Validity of Mean-Field Theory, Journal de Physique **44**, 775 (1983).
[16] T. W. Burkhardt, Propagator for the wetting transition in 1+1 dimensions, Phys. Rev. B **40**, 6987 (1989).
[17] D. B. Abraham, Solvable Model with a Roughening Transition for a Planar Ising Ferromagnet, Phys. Rev. Lett. **44**, 1165 (1980).
[18] D. B. Abraham, J. T. Chayes, and L. Chayes, Random Surface Correlation Functions, Comm. Math. Phys. **96**, 439 (1984).
[19] A. O. Parry, J. M. Romero-Enrique, and A. Lazarides, Nonlocality and Short-Range Wetting Phenomena, Phys. Rev. Lett. **93**, 086104 (2004).
[20] D. B. Abraham and D. A. Huse, Magnetization profile near a wall in the planar ising ferromagnet, Phys. Rev. B **38**, 7169(R)–7172(R) (1988).
[21] M. E. Fisher and B. Widom, Decay of Correlations in Linear Systems, J. Chem. Phys. **50**, 3756–3772 (1969).
[22] R. Evans, J. R. Henderson, D. C. Hoyle, A. O. Parry, and Z. A. Sabeur, Asymptotic decay of liquid structure - Oscilatory liquid-vapor density profiles and the Fisher-Widom line, Mol. Phys. **80**, 755 (1993).
[23] W. F. Saam, Wetting, Capillary Condensation and More, J. Low Temp. Phys. **157**, 77–100 (2009).
[24] M. E. Fisher and A. J. Jin, Effective Potential, Constraints, and Critical Wetting Theory, Phys. Rev. B **44**, 1430 (1991).

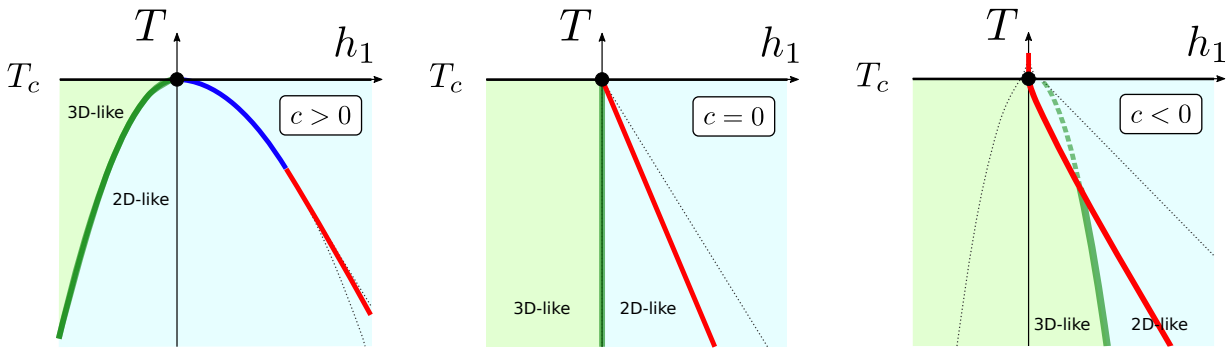


FIG. 1. Schematic illustration of sections of the Nakanishi-Fisher global surface phase diagrams in the (h_1, T) plane, for positive, zero and negative surface enhancements c and $h = 0^-$. The blue and red lines denote the critical and first-order wetting phase boundaries, respectively, with the thin dashed lines representing the spinodals. The green lines mark the 3D/2D crossover, separating regions where the correlation function decays with the 3D bulk correlation length (light green) from an interfacial region (light blue) where correlations are 2D-like and decay with a larger parallel correlation length. For $c < 0$, the lines of wetting and crossover meet so that, for $c < c_\dagger \approx -0.3375\,\kappa$, the 3D region extends up to the wetting transition. In this case, the extension of the crossover line (dashed green) into the metastable thin film region meets one of the spinodal lines at $T = T_c$.

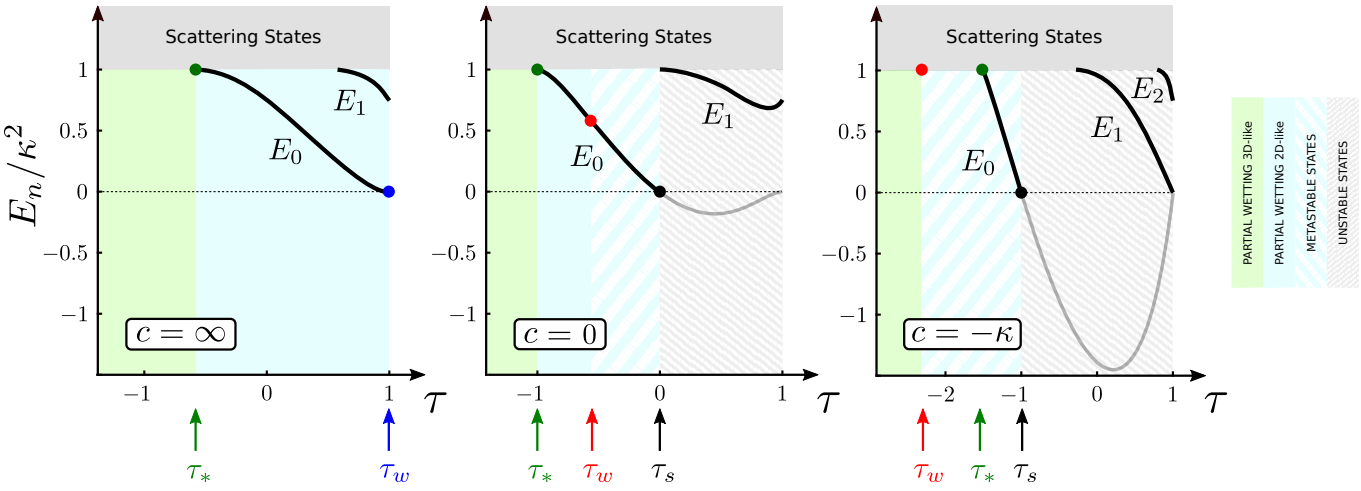


FIG. 2. Black and gray lines: Eigenvalue spectra determining the decay of correlations at the wall-fluid interface showing bound states (with $E/\kappa^2 < 1$) and scattering states (with $E/\kappa^2 > 1$) as a function of $\tau = m_1/m_0$ for critical wetting (illustrated here for $c = \infty$) and two types of first-order wetting ($c = 0$ and $c = -\kappa$). For critical wetting, the ground-state E_0 decreases monotonically from $E_0 = \kappa^2$ at the 3D/2D crossover ($\tau = \tau_*$, green dot) to zero at the wetting transition ($\tau = \tau_w = 1$, blue dot). For first-order wetting, E_0 vanishes at the spinodal ($\tau = \tau_s$, black dots). The regions corresponding to unstable, metastable and stable partial wetting films, which may be 3D-like or 2D-like, are also shown. For $c = -\kappa$, the 3D/2D crossover occurs before the wetting transition (red dot). Eigenvalues corresponding to higher bound states are shown, which meet the scattering band at non-thermodynamic singularities.

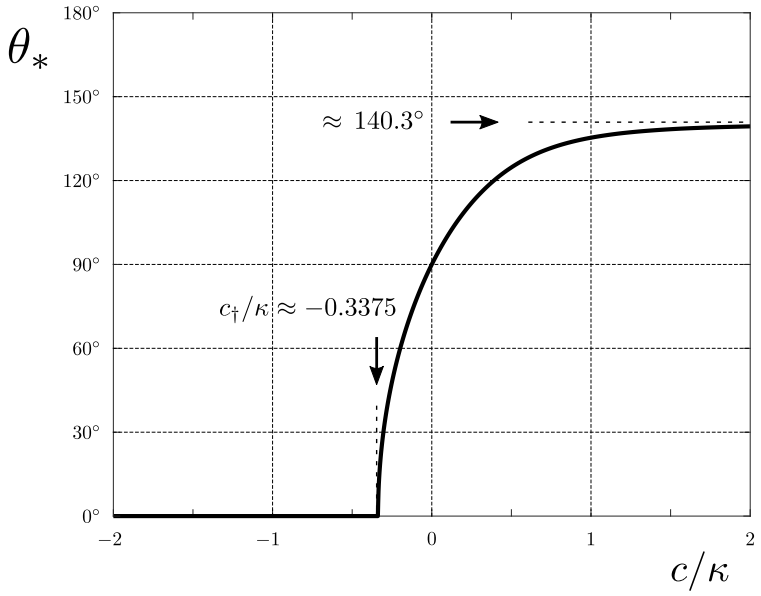


FIG. 3. The value of the equilibrium contact angle θ_* at the point of 3D/2D crossover as a function of the dimensionless parameter c/κ. For $c > 0$, the contact angle is large, since crossover occurs far from the wetting phase boundary, while for $c < 0$, pertinent to strongly first-order wetting transitions, the value of θ_* is small and vanishes for $c < c_\dagger \approx -0.3375\,\kappa$.

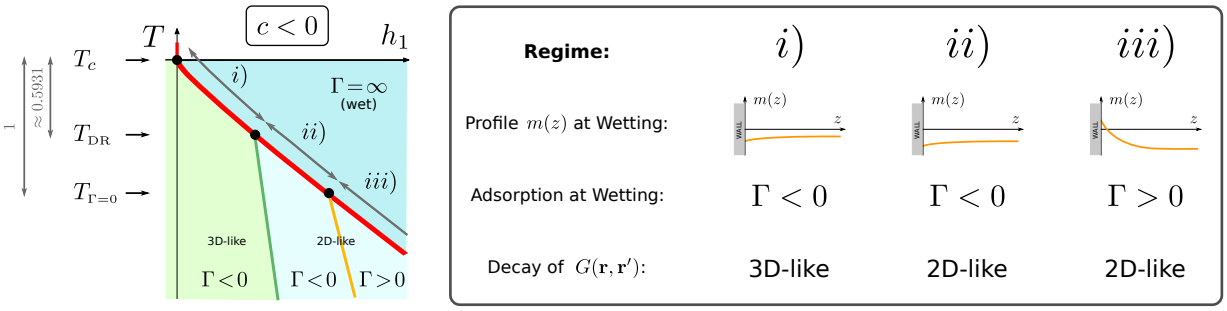


FIG. 4. Schematic wetting phase diagram for surface enhancement $c < 0$, showing the lines of first-order wetting (red), dimensional reduction (green), and the line of zero adsorption ($h_1 = -c\,m_0$) (orange). The lines of wetting and dimensional reduction cross at $T_{\rm DR}$, where the adsorption is negative. The adsorption along the wetting line increases as the wetting temperature is lowered, reaching $\Gamma = 0$ at $T_{\Gamma=0}$. This divides the wetting line into three different regimes with distinct characteristics, shown in the right-hand side: i), ii) and iii). The universal ratio between the shifts of the temperatures $T_{\rm DR}$ and $T_{\Gamma=0}$ from T_c in Eq. (4) is highlighted on the left hand side.